Osteocalcin-Controlled Dissolution−Reprecipitation of Calcium Phosphate under Biomimetic Conditions

Katharina Flade, Carsten Lau, Michael Mertig, and Wolfgang Pompe*

Institut für Werkstoffwissenschaft, Technische Universität Dresden, 01062 Dresden, Germany

Received February 13, 2001

We have examined the influence of osteocalcin, one of the 10 most abundant proteins of the human body, on hydroxyapatite (HAP, $Ca_{10}(PO_4)_6(OH)_2$) formation. Different functions in biomineralization are attributed to the bone-specific protein osteocalcin because of its Ca^{2+} binding including HAP binding properties and its capability to inhibit HAP precipitation. To study nucleation and crystal growth, a model system with osteocalcin-controlled dissolution−reprecipitation of brushite (DCPD, $CaHPO_4{\cdot}2H_2O$) to HAP has been investigated. After DCPD crystals were grown from aqueous solution, they were exposed to an osteocalcin-containing buffer solution of pH 7.4. Thin apatite-like crystals with hexagonal symmetry grew on the (010) brushite planes. The apatite (0001) planes were fully covered with osteocalcin molecules. Thus, osteocalcin has been found to regulate HAP formation in two different ways: (i) it accelerates nucleation, and (ii) it acts as a specific inhibitor of the apatite (0001) plane, supressing crystal growth perpendicular to this plane. A stress-induced growth model was developed illustrating HAP growth along the brushite−HAP interface considering compressions in the protein-covered HAP crystals.

Introduction

Until now the biomineralization process has not been completely understood.[1] For both medical reasons and fundamental understanding of hard tissue growth, one of the major goals is the clarification of the processes involved in bone mineralization. Different biomolecules (proteins and polysaccharides) are supposed to control biomineralization, and several control mechanisms for crystal growth are conceivable. Chemical and interfacial regulation of precipitation, matrix-induced or matrix-mediated nucleation and crystal growth, and inhibition by binding of molecules to specific faces of the crystal are the most important mechanisms which determine the crystal morphology. Interplay between stereochemical, structural, or electrostatic properties of a specific crystal face and the matrix governs the interaction of macromolecules and crystals in biomineralization.[2] Mineralization processes in biological systems, e.g., calcium carbonate formation in algae[3] or the deposition of crystalline phases with different morphologies on self-assembling acidic matrix molecules in aqueous solution,[4,5] have been the subject of several studies. With the same concept the biomimetic formation of inorganic compounds has been studied, using polymer templates[6,7] or self-assembled monolayers.[8]

The matrix of bone contains collagenous and noncollagenous proteins. Collagen serves as the scaffold within which the inorganic compound of bone, a calcium phosphate phase with great similarity in crystal structure to hydroxyapatite (HAP, $Ca_{10}(PO_4)_6(OH)_2$), is located. The gaps between the collagen fibrils are believed to provide nucleation sites when the bone minerals are formed. Several studies have examined HAP precipitation in collagen and other organic matrices.[9−12] Extensive studies have shown a strong influence of gelatine matrices on fluorapatite morphogenesis.[13]

Noncollagenous proteins are believed to be closely involved in the crystallization process too. Two mechanisms are assumed to be relevant: influence on the nucleation processes, and specific inhibition of crystal growth. Among the acidic proteins, synthesized by osteoblasts, only osteocalcin and bone sialoprotein are believed to be specific to mineralized tissues.[14]

The structure-controlling influence of these noncollagenous proteins on collagen mineralization has been mimicked by Bradt et al., using polyaspartic acid

(1) Boskey, A. L. *J. Cell. Biochem. Suppl.* **1998**, *30*, 83.
(2) Mann, S. In *Biomineralization: Chemical and Biochemical Perspectives*; Mann, S., Webb, J., Williams, R. J. P., Eds.; VCH: Weinheim, 1989; pp 35−62.
(3) Borowitzka, M. A. In *Biomineralization: Chemical and Biochemical Perspectives*; Mann, S., Webb, J., Williams, R. J. P., Eds.; VCH: Weinheim, 1989; pp 63−94.
(4) Levi, Y.; Albeck, S.; Brack, A.; Weiner, S.; Addadi, L. *Chem.−Eur. J.* **1998**, *4*, 389.
(5) Addadi, L.; Weiner, S. In *Biomineralization: Chemical and Biochemical Perspectives*; Mann, S., Webb, J., Williams, R. J. P., Eds.; VCH: Weinheim, 1989; pp 133−156.
(6) Antonietti, M.; Breulmann, M.; Göltner, Ch. G.; Cölfen, H.; Wong, K. K. W.; Walsh, D.; Mann, S. *Chem.−Eur. J.* **1998**, *4*, 2493.
(7) Falini, G.; Fermani, S.; Gazzano, M.; Ripamonti, A. *Chem.−Eur. J.* **1998**, *4*, 1048.
(8) Küther, J.; Nelles, G.; Seshadri, R.; Schaub, M.; Butt, H.-J.; Tremel, W. *Chem.−Eur. J.* **1998**, *9*, 1834.
(9) Du, C.; Cui, F. Z.; Zhang, W.; Feng, Q. L.; Zhu, X. D.; de Groot, K. *J. Biomed. Mater. Res.* **2000**, *50*, 518.
(10) Schwarz, K.; Epple, M. *Chem.−Eur. J.* **1998**, *4*, 1998.
(11) Moradian-Oldak, J.; Tan, J.; Fincham, A. G. *Biopolymers* **1998**, *46*, 225.
(12) Murphy, W. L.; Kohn, D. H.; Mooney, D. J. *J Biomed. Mater. Res.* **2000**, *50*, 50.
(13) Busch, S.; Dolhaine, H.; DuChesne, A.; Heinz, S.; Hochrein, O.; Laeri, F.; Podebrad, O.; Vietze, U.; Weiland, Th.; Kniep, R. *Eur. J. Inorg. Chem.* **1999**, 1643.
(14) Hunter, G. K.; Hauschka, P. V.; Poole, A. R.; Rosenberg, L. C.; Goldberg, H. A. *Biochem. J.* **1996**, *317*, 59.

10.1021/cm011063z CCC: $20.00
Published on Web 09/19/2001

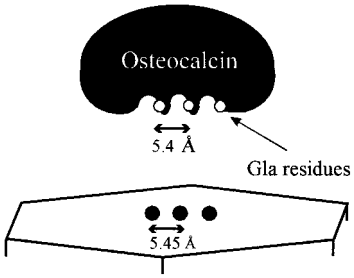

Figure 1. Schematic representation of the osteocalcin−HAP interaction. Ca^{2+} ions are represented as black dots. The corresponding distances between Gla residues of osteocalcin and Ca^{2+} sites of the HAP (0001) planes, respectively, are indicated. (Redrawn from ref 16.)

and polyglutamic acid as model substances for acidic proteins.[15]

In bone, osteocalcin (bone γ-carboxyglutamic acid protein, Gla protein) is the predominant Gla protein with contributions up to 20% of noncollagen bone tissue proteins. It has revealed itself as a highly specific osteoblastic marker produced during bone formation.[16] A detailed review on osteocalcin has been given in the paper of Hauschka. The osteocalcin molecule contains 46−50 amino acid residues and has a molecular weight of 5200−5900. Conformational studies have shown that osteocalcin consists of α-helical and β-sheet structures. Two antiparallel α-helices, the "Gla helix" (residues 16−25) and the "Asp-Glu helix" (residues 30−41), are framed by β-sheet structures. Because of its content of three Gla residues in each molecule, osteocalcin has a strong Ca^{2+} binding effect. The carboxyl groups of Gla residues are the main binding sites for Ca^{2+}. In this interaction only 2 of 6−9 coordination sites of Ca^{2+} are occupied, so Ca^{2+} can interact with further ligands. Therefore, it can be presumed that osteocalcin interacts with Ca^{2+} in the HAP crystal lattice in bone also. Hauschka has proposed a model which reflects the crystallographic correspondence of the osteocalcin and particular lattice planes of the HAP crystal (Figure 1, ref 16). The very special property of the Gla helix is the regular spacing of the three charged Gla residues at intervals of three or four residues (e.g., residues 17, 21, and 24) with hydrophobic residues between them. Because of the Gla helix 3.6 residues/turn, the α-helix has an amphipathic character with both anionic and hydrophobic surfaces. The α-helix has a periodicity of 5.4 Å, which is remarkably similar to the interatomic lattice spacing of Ca^{2+} in the (0001) planes of HAP, which is 5.45 Å. Hauschka suggested a specific adsorption of osteocalcin to these surfaces. Experimental evidence for this assumption has not been found until now. The important question is whether the crystal growth perpendicular to the (0001) HAP planes is inhibited by specific adsorption of osteocalcin molecules.

In search of the functional aspect in biomineralization, osteocalcin is further assumed to be an inhibitor of HAP precipitation. Recently, nucleation and inhibition activity of osteocalcin on HAP was studied over a wide range of osteocalcin concentration.[14] At concentrations up to 10 μg/mL osteocalcin was found to mainly delay nucleation. The minimum concentration to cause a nucleation effect was determined as 100 μg/mL. Addition of osteocalcin to the liquid precursor for preparation of HAP−collagen composites causes a significant change of the morphology of the HAP nanocrystals.[17]

In the present study, we have directly observed the first stages of HAP growth controlled by osteocalcin by scanning force microscopy (SFM). However, nanosize specimens with high porosity resulting from conventional precipitation processes are not suitable for SFM measurements. Therefore, we developed a model system using an osteocalcin-controlled dissolution−reprecipitation process of brushite (DCPD, $CaHPO_4{\cdot}2H_2O$) to HAP. Brushite crystals form a smooth (010) surface which allows the imaging of HAP formation on brushite. Dissolution−reprecipitation of calcium phosphates can be controlled by their pH-dependent solubilities.[18] At room temperature and pH values below 4.2, DCPD is the most stable calcium phosphate, whereas above 4.2, HAP is preferentially formed. When DCPD is exposed to a solution with a pH value above 4.2, the more stable calcium phosphate HAP will reprecipitate. Although the solubilities of DCPD and HAP are very low, the solubility of DCPD is higher than that of HAP under such conditions. Therefore, HAP formation occurs very slowly. However, in the presence of osteocalcin we found the nucleation is accelerated. At the same time osteocalcin inhibits HAP crystal growth by adsorbing specifically to the (0001) face of apatite crystals. Direct imaging of the protein−crystal interaction is possible by SFM. The experiments verify the idea of a strong crystallographic coupling of osteocalcin adsorption and the HAP structure as developed by Hauschka.[16]

Experimental Section

Materials. Osteocalcin from bovine bone was purchased from Calbiochem-Novabiochem GmbH (Germany). Osteocalcin was dissolved in protein buffer (pH 7.4) at a concentration of 4 mg/mL containing 10 mmol/L sodium phosphate and 75 mmol/L NaCl. For fluorescence analysis the marker TAMRA (5(and 6)-carboxytetramethylrhodamine, succinimidyl ester, 5(6)-TAMRA, SE) was used (Molecular Probes, Inc.).

Synthesis of Brushite. A 2.5 mL sample of 0.15 M $CaCl_2$ was mixed with 45 mL of distilled water in a Petri dish. Subsequently, 2.5 mL of 0.1 M Na_2HPO_4 was added to the $CaCl_2$ solution to receive a total volume of 50 mL. The final concentrations were 7.5 mmol/L $CaCl_2$ and 5 mmol/L Na_2HPO_4. The crystal growth experiment was performed at 20 °C. After 4 weeks, grown crystals were filtered off, rinsed with distilled water, and dried with nitrogen. The final pH of the solution was 5.5.

X-ray Diffraction. For the X-ray diffraction the DCPD crystals were ground before the measurement. The diffraction measurements were performed with a D 500 diffractometer (Siemens). Co Kα radiation was applied.

Imaging of Single Osteocalcin Molecules. To demonstrate the satisfying resolution for osteocalcin, single osteocalcin molecules were imaged with the scanning force microscope on a mica surface. A freshly cleft mica surface (1 cm^2)

(15) Bradt, J.-H.; Mertig, M.; Teresiak, A.; Pompe, W. *Chem. Mater.* **1999**, *11*, 2694.

(16) Hauschka, P. V.; Lian, J. B.; Cole, D. E. C.; Gundberg, C. M. *Physiol. Rev.* **1989**, *69*, 990.

(17) Knepper-Nicolai, B.; Reinstorf, A.; Hofinger, I.; Wenz, R.; Pompe, W. Submitted to Symposium G: Cell-Biosystem Material Interactions, European Materials Research Society Spring Meeting, Strasbourg, June 2001.

(18) Elliott, J. C. *Structure and Chemistry of the Apatites and other Orthophosphates*; Elsevier Science B.V.: Amsterdam, 1994.

was prepared. A 20 μL sample of a 10 mM $CaCl_2$ solution was dropped onto the mica surface. After incubation for 10 min in a closed Petri dish, covered with damp filter paper, the mica surface was rinsed with 3 mL of distilled water. The osteocalcin solution was diluted with protein buffer (pH 7.4) to reach a protein concentration of 25 μg/mL. A 10 μL sample of this osteocalcin-containing solution was added to the mica surface and incubated for 8 min. Afterward the specimen was rinsed with 3 mL of distilled water and dried with nitrogen.

Dissolution−Reprecipitation Experiments. Dissolution−reprecipitation experiments were carried out at pH 7.4 and 25 °C. The osteocalcin solution (4 mg/mL) was diluted with protein buffer (pH 7.4) containing 10 mmol/L sodium phosphate and 75 mmol/L NaCl to reach a protein concentration of 0.25 mg/mL. A 5 μL sample of this osteocalcin-containing solution was dropped onto the DCPD crystals (area up to 10 mm^2) for the protein-controlled dissolution−reprecipitation. For osteocalcin-free dissolution−reprecipitation 5 μL of protein buffer (pH 7.4) was dropped onto the DCPD crystals. The solutions were incubated for 5 min, 1 h, and 2 h. Subsequently the DCPD crystals were rinsed with 5 mL of distilled water and dried with nitrogen.

Scanning Force Microscopy. SFM was performed with a commercial multimode microscope (NanoScope IIIa, Digital Instruments) operated at ∼300 kHz in tapping mode under ambient environmental conditions. The scan rate was ∼1 line s^{-1}, and scanning was performed with silicon tip cantilevers (NanoProbe, 125 μm) at a minimum tapping force. DCPD crystals were imaged before the dissolution−reprecipitation experiments and after various incubation periods of protein-containing and protein-free solution. The images shown in this paper display height mode or amplitude mode. The amplitude signal is simultaneously recorded with the height signal. The amplitude signal is analoguous to the deflection signal in the conventional error mode[19] and especially allows for resolution of small corrugations of the sample surface.

Fluorescence Analysis. TAMRA was dissolved in dimethyl sulfoxide (DMSO) at 10 mg/mL immediately before the reaction was started. The TAMRA-containing solution was mixed with 0.1 M sodium bicarbonate in a ratio of 1:10. The pH value of the sodium bicarbonate buffer was 8.3. A 3 μL sample of TAMRA-containing solution was added to the DCPD crystal after the protein-controlled dissolution−reprecipitation experiment to detect osteocalcin. The solution was incubated for 1 h at room temperature in darkness. Subsequently, the sample was rinsed with distilled water. Fluorescence microscopy was performed with an Axiovert 100M (Zeiss). The absorption maximum of TAMRA is 555 nm, and the fluorescence emission maximum is 580 nm. Three different types of specimens were investigated: DCPD crystals before the dissolution−reprecipitation experiment, and partially transformed crystals after incubation in protein-containing and protein-free solution.

Results

Crystallization of Brushite. In the crystallization experiment large platelike crystals grew with a length up to 5 mm and an area up to 10 mm^2. The crystallographic structure of the grown crystals was studied with X-ray diffraction. The X-ray diffraction pattern showed typical peaks for DCPD with the preferred orientation (010). The most intensive peaks were the (020), (040), and (060) peaks; in addition there were weaker peaks, (021), (041), and (061).

Imaging of Single Osteocalcin Molecules. With the applied SFM method, imaging of single osteocalcin molecules deposited on smooth surfaces is possible. The osteocalcin molecules were randomly distributed on the mica surface as can be seen in Figure 2. The height of the osteocalcin molecules was measured to be 2.7 nm, which reasonably agrees with the proposed structure model of the molecule. However, the measured width of the protein is expected to be a bit distorted because of capillary forces and the tip radius of the cantilever.

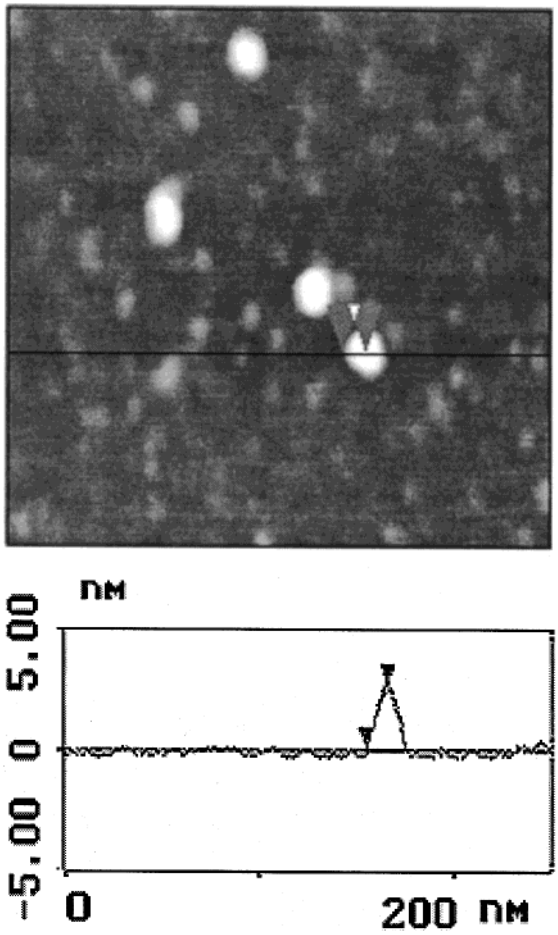

Figure 2. Height profile of a mica-deposited osteocalcin molecule (markers indicate a difference of 2.7 nm).

Dissolution−Reprecipitation Experiment without Osteocalcin. After incubation of the protein-free buffer solution (pH 7.4) to DCPD crystals for 5 min, 1 h, and 2 h, no structure transformation from DCPD to HAP was found. SFM measurements did not show any changes of the (010) DCPD plane after 5 min of buffer incubation (Figure 3). Even 1 or 2 h of incubation of protein-free buffer did not cause any dissolution−reprecipitation process.

Osteocalcin-Controlled Dissolution−Reprecipitation. After 5 min of incubation with protein-containing buffer, the lattice steps on the (010) DCPD plane were covered with small spheres as detected by SFM measurements (Figure 4). Subsequent fluorescence measurements have proven that these spheres are osteocalcin molecules. Osteocalcin molecules stuck to the lattice steps only, not to the (010) planes of DCPD. The height of a single osteocalcin molecule adsorbed to DCPD was found to be about 1.9 nm by SFM section analysis.

As seen with SFM after 1 h of incubation of osteocalcin-containing buffer, thin hexagonal crystal plates were grown on the (010) DCPD plane (Figure 5). All thin

(19) Putman, C. A. J.; van der Werf, K. O.; de Grooth, B. G.; van Hulst, N. F.; Greve, J.; Hansma, P. K. *Proc. SPIE* **1992**, *1939*, 198.

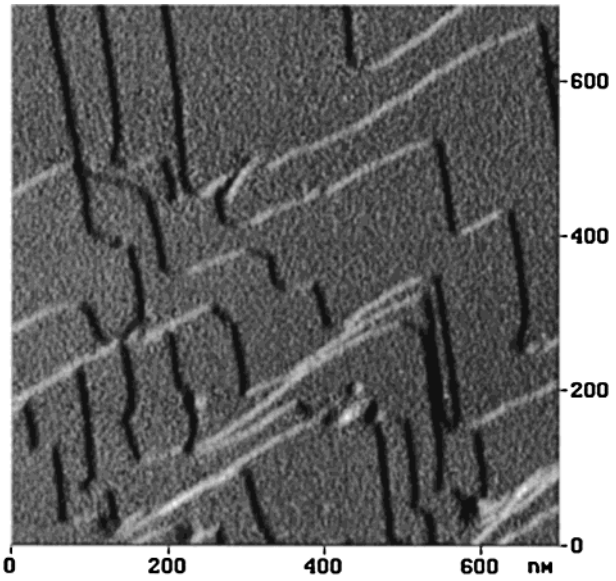

Figure 3. SFM image of DCPD (010) faces showing single ledges (amplitude image).

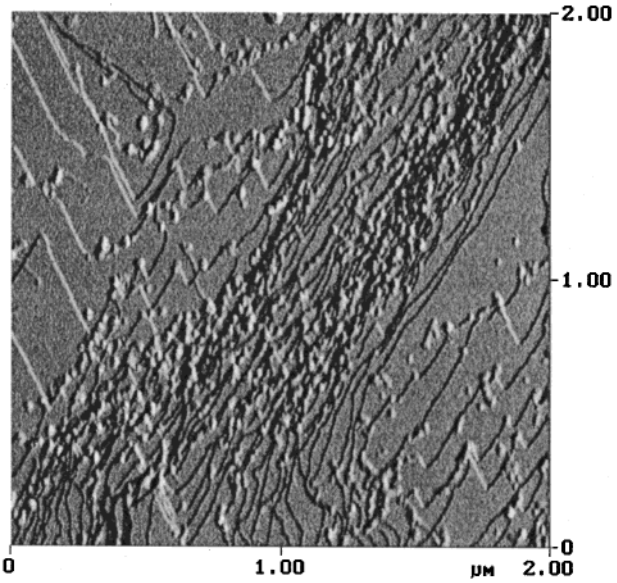

Figure 4. SFM image of DCPD (010) faces after 5 min of incubation with osteocalcin-containing buffer. Osteocalcin molecules adsorbed only to the lattice steps (amplitude image).

plates were closely beset with small spheres, but there were no spheres on the DCPD surface except along the ledges of the (010) plane. It was shown later that these thin hexagonal crystals were fully covered with osteocalcin. The platelets were partially so thin and flexible that lattice steps from the DCPD substrate were still detectable on their surface.

As shown with SFM measurements and section analysis, crystal monolayers grew during the structure transformation process. Later the platelets came into mutual contact. The grown crystal areas were of 2−20 μm diameter. After a 2 h incubation of the osteocalcin-containing solution, the DCPD surface was covered with platelets of hexagonal symmetry (Figure 6). In addition, the apatite-like plates showed an interesting growth pattern. Lattice planes of the hexagonal crystal plates piled up parallel to the edges. Emerging ledges were always staggered with similiar distances of about 50−200 nm, and they were covered with osteocalcin molecules.

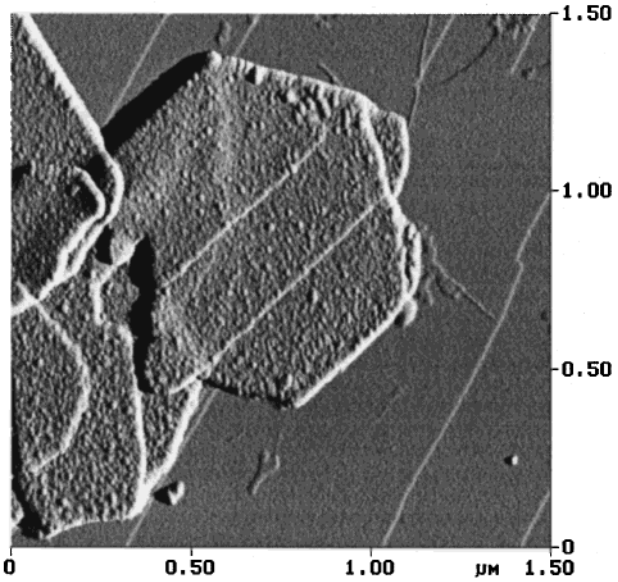

Figure 5. SFM image of precipitated hexagonal, apatite-like crystals on the DCPD (010) face after 1 h of incubation with osteocalcin-containing buffer. Only the apatite-like crystals are covered with osteocalcin molecules (amplitude image).

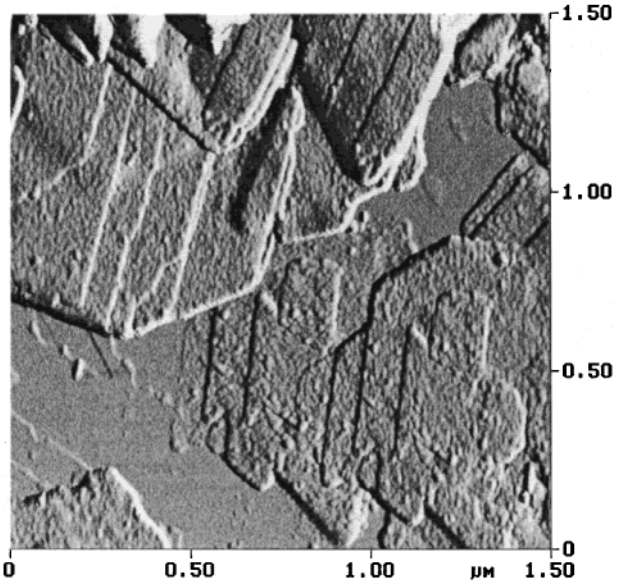

Figure 6. SFM image of precipitated apatite-like crystals on the DCPD (010) face after 2 h of incubation with osteocalcin-containing buffer. Crystal ledges arrange themselves parallel to the (1100), (0110), and (1010) directions with mutual distances (amplitude image).

Fluorescence Analysis. Because osteocalcin was the only protein present in the experiments, a nonspecific protein marker, TAMRA, could be used for osteocalcin detection. As described before, the osteocalcin-controlled dissolution−reprecipitation process resulted in growth of hexagonal plates tightly packed with small spheres. All these plates fluoresced after treatment with the nonspecific protein marker TAMRA (Figure 7). Single lattice steps on the (010) DCPD plane were not visible by light microscopy, but large numbers of closely adjoining steps were. After treatment with TAMRA, fluorescence was also found along these close-packed ledges.

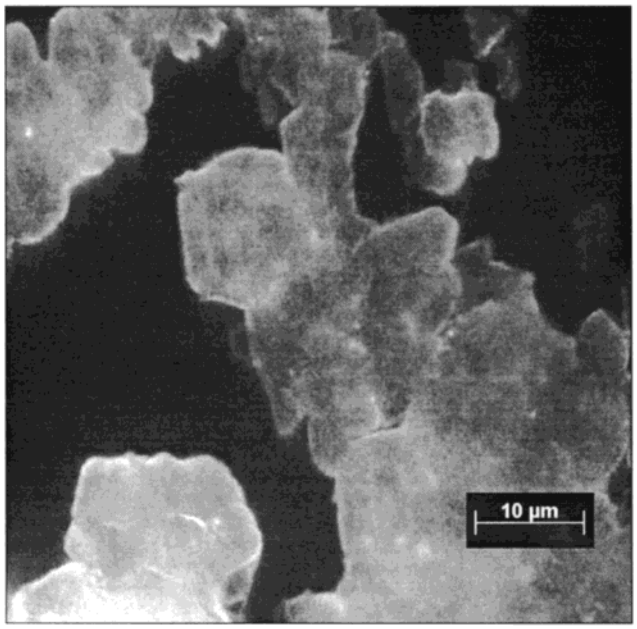

Figure 7. Fluorescence micrograph of osteocalcin-covered apatite-like crystals on the DCPD surface after treatment with the nonspecific protein marker TAMRA. DCPD does not show any significant fluorescence.

Apart from the grown hexagonal plates and the ledges, no fluorescence occurred on the DCPD (010) plane. Accordingly, no fluorescence occurred after treatment with TAMRA of fresh DCPD specimens and those incubated with a protein-free solution.

Discussion

Imaging of Osteocalcin on Mica and on DCPD Single Crystals. With 46−50 amino acid residues, osteocalcin is a very small molecule, and only SFM enables direct imaging. With its atomically flat surface, mica represents a well-suited substrate for SFM imaging of biomolecules.

The conventional method to examine the nucleation and inhibition activity of osteocalcin during the formation of HAP would be the direct precipitation of HAP from aqueous solutions with added protein. However, SFM imaging of precipitated nanosize HAP crystals was problematic. This has been circumvented by the dissolution−reprecipitation transformation of DCPD to HAP owing to the characteristic layered structure of DCPD. The DCPD crystal structure is monoclinic with space group *Ia*, with lattice parameters $a = 5.812$ Å, $b = 15.180$ Å, $c = 6.239$ Å, and $\beta = 116° 25'$.[18] The DCPD structure consists of two bilayers parallel to the (010) plane. One bilayer presents sheets of calcium and phosphate ions, the other bilayer is formed by water molecules, and both bilayers alternate with the *b* axis as surface normal. Because of its platelike morphology in the (010) orientation, it is very suitable for atomic force microscopy. Figure 3 shows single steps of the DCPD lattice on the (010) face. The distance between two planes separated by one step is 7.6 Å, which is half the lattice parameter *b* of DCPD, as can be seen in Figure 8. The orientation of the ledges agrees with characteristic orientations of DCPD planes. The hydrated layer is the terminating layer at the surface of the (010) face in aqueous solutions. This behavior is due

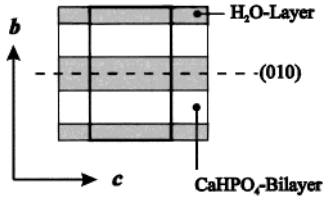

Figure 8. Schematic representation of DCPD viewed on the (100) plane, showing the water and $CaHPO_4$ bilayers.

to the much higher concentration of water molecules in the solution compared to those of calcium and phosphate ions. Therefore, the calcium phosphate motif of the (010) plane is not able to interact with macromolecules.[20] Our SFM examinations confirmed this statement. After 5 min of incubation of osteocalcin-containing buffer with a pH value of 7.4, osteocalcin adsorption was observed just at the ledges but not on the (010) plane of DCPD (Figure 4). Only at the ledges the (010) water layer is interrupted, and there the calcium and phosphate ions are able to interact with osteocalcin molecules. It should be assumed that the interaction of osteocalcin with the exposed Ca^{2+} along DCPD ledges plays an important role in the subsequent structure transformation.

Dissolution−Reprecipitation Mechanism. It was mentioned before that both DCPD and HAP have a low solubility at a pH value of 7.4. Under normal conditions, the structure transformation is connected with dissolution and precipitation. Therefore, the transformation is a very slow process. So it is not surprising that no reprecipitation was observed when DCPD was exposed to the protein-free buffer with pH 7.4 for 2 h. Contrary to this, the observed reprecipitation after exposure to osteocalcin-containing buffer for 1 h is remarkable. With a protein concentration of 0.25 mg/mL, osteocalcin accelerated the nucleation. This confirms previous observations that the minimum concentration required for nucleation is 0.1 mg/mL, and that osteocalcin delays nucleation up to 10 μg/mL.[14]

The grown crystals were very thin and partly monolayers. These thin plates had a hexagonal shape with typical angles of 120° between the (1100), (0110), and (1010) planes and a striking similiarity to the apatite structure. Lattice parameters of HAP are $a = b = 9.432$ Å, $c = 6.881$ Å, and $\gamma = 120°$.[18] The height difference between two protein-covered HAP planes was measured as 0.7−1.5 nm. This compares to the lattice parameter $c = 6.881$ Å. The (0001) planes of the grown hexagonal prism were parallel to the (010) planes of DCPD. We have been able to show that osteocalcin adsorbs specifically to the (0001) plane of the grown hexagonal apatite-like plates, which is a direct verification of the interaction model of osteocalcin with Ca^{2+} in the HAP lattice proposed by Hauschka.[16] Obviously proteins inhibited the growth perpendicular to the (0001) plane. To our knowledge this is the first direct imaging of a growth-limiting absorption of proteins to a calcium phosphate crystal plane.

Osteocalcin-Controlled Growth Model with Stress-Induced Pattern Formation. The osteocalcin-controlled HAP dissolution−reprecipitation from DCPD can be summarized in a four-step model.

(20) Moradian-Oldak, J. Ph.D. Dissertation, Weizmann Institute, Rehovot, Israel, 1992.

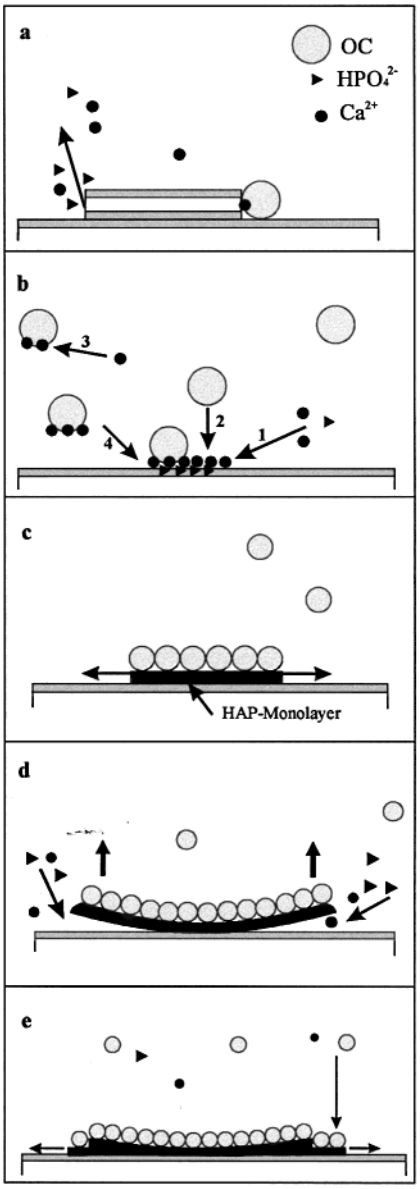

Figure 9. Four-step model for the dissolution−reprecipation mechanism of DCPD to HAP under the influence of osteocalcin. The main steps are dissolution of DCPD (a), osteocalcin-activated nucleation of HAP on the DCPD (010) face (b), lateral growth of HAP crystals by blocking the (0001) HAP face by osteocalcin (c), stress-induced delamination along the water−HAP interface, and further HAP formation in the developed thin gaps at the water apatite interface, resulting in a characteristic growth pattern (d, e).

(a) DCPD Dissolution. In the first stage the DCPD (010) plane is exposed to the osteocalcin-containing buffer with a pH value of 7.4. Under these conditions, DCPD is no longer thermodynamically stable and dissolution of DCPD begins at the ledges. Simultaneously osteocalcin molecules are taken up by the exposed lattice steps on the (010) plane of the DCPD crystal (Figure 9a). Just there interaction of the protein with the calcium phosphate motif of DCPD is possible.

(b) Osteocalcin-Activated Nucleation. The next step is nucleation of the more stable apatite phase (Figure 9b). As described before, growth of apatite crystals was only observed after incubation with osteocalcin-containing buffer solution. Consequently this protein activates the nucleation process. We assume that osteocalcin molecules adsorbed at the ledges of the DCPD (010) plane act as apatite nucleation centers because the Gla helix of one osteocalcin molecule has three binding sites for Ca^{2+}, and the periodicity of the osteocalcin α-helix (5.4 Å) is similar to that of the hexagonally arranged Ca^{2+} in the (0001) plane of the HAP lattice.[16] Dissolved calcium and phosphate ions bind to this template and form the first monolayer as a (0001) plane with hexagonal structure (Figure 9b, arrow 1). Because of their binding specificity for the (0001) plane of HAP, osteocalcin molecules cover immediately the grown (0001) apatite monolayer (arrow 2). Another mechanism is also possible and could take place simultaneously. Because of the high osteocalcin concentration, proteins bind Ca^{2+} in free solution (arrow 3) so that HAP nucleation takes place in aqueous solution. Subsequently bonds are formed to an existing HAP monolayer on the (010) DCPD plane (arrow 4).

(c) Osteocalcin-Terminated Layer Growth. In the following stage a (0001) hexagonal apatite monolayer grows on the (010) DCPD plane (Figure 9c). The tight covering with protein inhibits the (0001) HAP plane and prevents growth perpendicular to the (0001) plane. Therefore, crystal growth of the monolayer takes place only at the (1100), (0110), and (1010) planes of HAP. Due to the DCPD subnanometer water layer, there should be a significant contribution of van der Waals interaction that favors growth along this plane in addition to the enrichment of calcium and phosphate near the DCPD surface. However, there is no crystallographic control of the growing HAP layer by the underlying DCPD crystal. The crystallography and shape of the HAP layer are only determined by the inhibiting effect of the osteocalcin layer.

(d) Stress-Driven Patterning. As mentioned before, grown apatite platelets develop a special growth pattern where crystal ledges arrange themselves parallel to the (1100), (0110), and (1010) directions with similar mutual distances. Although osteocalcin has an adsorption specificity for the (0001) plane of HAP and distances between Gla residues (5.4 Å) are similar to the interatomic distances of Ca^{2+} in the (0001) plane of HAP (5.45 Å), the protein layer does not perfectly fit the crystal monolayer. The misfit of 1% could be the reason for the change of the layer growth mode similar to the famous Stranski−Krastanov model describing the transition from layer to island growth. Following this model, we assume that the increasing stored elastic energy is the driving force for the growth mode change. However, here we have to consider the particular situation of an almost inhibited top surface of the growing layer. The observed staggered layer pattern can be explained by considering the particular residual stress distribution and the stored elastic energy in the growing two-layer structure of osteocalcin and HAP. For simplicity we assume that this thin layered structure is very weakly attached to the terminating water layer of DCPD. With the mentioned data for the Gla residue distance and the Ca^{2+} distance in the (0001) plane of HAP, it can be assumed that the protein layer is under tension whereas the growing HAP layer is compressed. The residual stresses increase with increasing length L of the growing osteocalcin-covered HAP crystal. These stresses could relax by bending the growing composite layer as shown in Figure 9d.

We assume a layer thickness D of the osteocalcin−HAP composite film. As a precondition for delamination, the elastic energy per layer area of the osteocalcin−HAP composite $\eta_{el}D = (\sigma_{mis}^2/E)D$ has to exceed the increase of the interface energy change $\Delta\gamma_{in}$ between the HAP layer and the DCPD (010) plane due to crystallization of a new HAP interlayer. Here σ_{mis} stands for the characteristic compressive residual stress (−) in the HAP film and the tensile residual stress (+) in the osteocalcin film. E is a characteristic average stiffness estimate of both films. From a very simple micromechanical model it can be derived that there should be a length L of the growing osteocalcin−HAP composite layer when ledges of the apatite platelets lift off. To build up the full residual stresses in the bilayered system, a minimum extension of the layer is necessary. Suppose that the stresses between the osteocalcin film and the HAP film are transferred by shear with a characteristic yield stress τ_s. Then the scaling of the increase of the residual stresses with the layer extension L can be described in the so-called shear lag approximation as $\sigma_{mis}/\tau_s = L/D$. When we assume the following values for the characteristic parameters in the micromechanical model, $D = 1$ nm, $\tau_s = 0.1$, ..., 1 Mpa, and $\Delta\gamma_{in}E = 10^{-2}$ MPa^2 m, delamination should occur when the film has an extension of $L = 15$, ..., 1.5 μm, where the higher L value relates to the smaller yield stress.

Further HAP formation takes place in the developed thin gaps at the DCPD−HAP interface (Figure 9e). During growth of the new HAP crystals, specific inhibition by osteocalcin acts again and growth is possible only as a monolayer until the critical size L is reached again. Thus, this favored growth at the DCPD water layer−apatite interface is connected with a characteristic growth pattern.

Conclusions

The effect of osteocalcin on hydroxyapatite formation has been investigated in several studies elucidating the nucleation and inhibition functions of the bone-specific protein. In the present study the Hauschka model for interaction of osteocalcin with Ca^{2+} in the hydroxyapatite lattice was taken up. Studying a dissolution−reprecipitation process from brushite to hydroxyapatite under biomimetic conditions, we have found an experimental proof for the assumed nucleation and inhibiting effect of osteocalcin. By SFM measurements the osteocalcin activity during DCPD dissolution and HAP precipitation has been imaged directly. We observed an effect on HAP nucleation, especially an osteocalcin-induced acceleration of the dissolution−reprecipitation process. At the same time SFM and fluorescence measurements showed the inhibiting function of the protein on the growing apatite-like crystals. Osteocalcin interacts specifically with the (0001) plane of the grown apatite phase, and subsequently the proteins inhibit crystal growth perpendicular to this plane. A staggered pattern of growing layers has been observed which can be explained by a growth stress-controlled mechanism. Crystal growth parallel to the (0001) plane induces stresses in the protein−HAP bilayer, which can relax by nucleation of a new sublayer along the DCPD−water bilayer in the (010) orientation. In summary our studies showed that osteocalcin has a 2-fold influence on the formation of hydroxyapatite. This confirms the assumption that osteocalcin is one important part in the hierarchy of regulatory components in bone mineralization. Further work with the SFM liquid cell will enable examination of protein-controlled HAP formation under physiological conditions.

Acknowledgment. We express our sincere gratitude for financial support on behalf of the DFG grant for the research group “Investigation of the interaction between biological interfaces of medical implants and living organisms”, FOR 308/2-1. We also thank M. Gelinsky, B. Knepper-Nicolai, S. Matys, A. Reinstorf, and M. Witt, Technische Universität Dresden, and H. J. Weiss for many fruitful discussions.

CM011063Z